Microwave generation in a high voltage triggered pseudospark discharge experiment

K. Ramaswamy, W. W. Destler,[a] and J. Rodgers
Electrical Engineering Department and Institute of Plasma Research, University of Maryland, College Park, Maryland 20742

(Received 2 January 1997; accepted for publication 3 December 1997)

A set of five experiments to study the microwave emission accompanying the high voltage pseudospark discharge are reported. The generation of the microwaves in all cases but one is attributed to electron beam-plasma interaction. In the other case, Cherenkov radiation was also considered as a possible mechanism of generation. Initial simulation studies were carried out which predict a background peak plasma density on the order of $1-2\times10^{13}\text{cm}^{-3}$. © *1998 American Institute of Physics.* [S0021-8979(98)03106-5]

I. INTRODUCTION

The pseudospark discharge is a low pressure gas discharge in a hollow cathode and a planar anode configuration operating on the left-hand branch of a characteristic breakdown curve which is similar to the Paschen curve for parallel electrodes. This phenomenon was first reported by Christiansen and Schultheiss.[1] The pseudospark discharge has several interesting features. One important feature has been the observance of highly pinched electron beams with current densities of up to 10^6 A/cm^2 during the breakdown phase.

A high voltage (300–400 kV) pseudospark experiment was designed and executed with the intent of eventually extracting these ion-focused electron beams into vacuum. Generating electron beams at these high energies was intended to reduce the self-space charge fields. The pseudospark discharge was accompanied by a wide variety of microwave signatures.

It is of great interest to investigate the interaction of an electron beam with the plasma formed as a result of ionization collisions of beam electrons with molecules of a neutral gas in the absence of a magnetic field. This study may be important in the development of a physical model to describe the processes which accompany the polar aurora formation.[2]

While there have been other experiments[2–4] to investigate the microwave radiation accompanying the passage of the electron beam through low pressure gas, the pseudospark experiment reported here is different in the following manner.

In a pseudospark device, electron beam generation and propagation through a gas filled environment are closely coupled. In other experiments, a monoenergetic electron beam was generated first and then introduced in a gas filled drift tube. In the case of the pseudospark discharge, the energy of the ejected electron beam is a function of the anode-cathode voltage wave form and therefore, a function of time. The electron beam is generated in a self-pinched manner. The typical dimensions of the electron beam (operating voltage 370–400 kV) lie in the range of 4–0.5 mm.[5,6] The higher energy electrons are not pinched and the electron beam has a diameter of 4 mm. The pinched lower energy electron beam (generated later in time) has a diameter of the order of 0.5 mm. The pinched electron beam is associated with a growing background plasma. The plasma produced by the beam is narrow and inhomogeneous.

Although microwave emissions have been observed previously in a pseudospark experiment[7] (a back-lit thyratron), the high voltage pseudospark experiment reported here differs in the following manner.

(i) Microwave emission was observed directly on axis on the anode side in contrast to the back-lit thyratron experiment, where it was observed on the cathode side.
(ii) The voltage of operation of the device was much higher. In the case of the back-lit thyratron, the voltage of operation was on the order of 20 kV.
(iii) In the case of the back-lit thyratron experiment, microwave emissions were observed in the frequency range (20–100 Ghz) whereas in the triggered high voltage pseudospark experiment, microwaves were mostly observed in the frequency range 8–33 GHz.

Initial experiments to investigate the microwave emissions are reported in this paper. The paper is organized as follows. Section II deals with the experimental setup, Sec. III contains a description of the experiments, and in Sec. IV, the experimental results are discussed and finally the conclusions from the experiments are drawn in Sec. V.

II. EXPERIMENTAL SETUP

The experimental setup for the high voltage pseudospark is shown schematically in Fig. 1. The apparatus has been described elsewhere.[6] A quasi-dc (long pulse 35 μs), high voltage (500 kV), unipolar pulse is applied to the cathode through a charging resistor of 9 kΩ. The trigger system design helps the initiation of the discharge by providing a small flashover between the trigger electrode and the surrounding wall of the cathode. A six gap multistack system was chosen with an aperture size of 0.635 cm, insulator thickness (gap

[a]Electronic mail: destler@eng.umd.edu

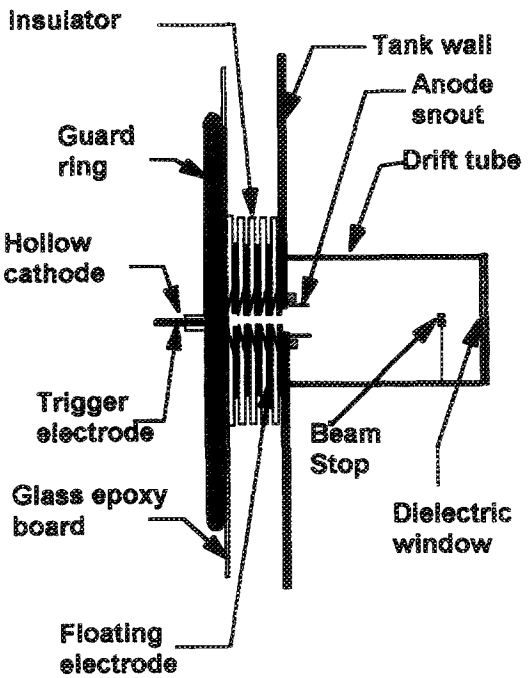

FIG. 1. High voltage triggered pseudospark setup. Side view of the multistack pseudospark with the external capacitor and trigger circuit. This setup was used for experiments 1 and 2.

distance) of 1.3 cm, where the thickness of the individual electrodes was 0.32 cm. The diameter of the electrode was 7.62 cm and the diameter of the insulator was 9.53 cm. The reason for this small diameter was the ease of fabrication of the insulators and floating electrodes. To boost the capacitance of the system, a low inductance parallel plate capacitor was used. One plate was directly attached to the cathode and the tank wall formed the other plate. The plate that was attached to the cathode was made out of a glass epoxy (G10) board, with the copper stripped from the side facing the tank. The total capacitance of the system was 80 pF.

A. Diagnostics

An exit wall current monitor (a fast current transformer) was used to measure the total electron current ejected out from the downstream end of the device. A Faraday cup was also used to measure the total beam current as a function of distance along the system axis. A capacitive voltage divider monitors the voltage at the output of the transformer and a $\dot{D}$ probe monitors the pseudospark voltage. A Pirani gauge was used to measure the ambient gas pressure in all experiments. The microwave measurements were carried out on axis. Microwaves broadcast into free space from the output window (made of plexiglass) were collected by a pyramidal horn (X brand/K band), carried into a screen room by waveguide pipelines (X band/K band) where they were rectified by crystal detectors.

III. EXPERIMENT

A series of five preliminary experiments were carried out. The voltage of operation was between 350 and 400 kV and discharge took place on command with the help of an external trigger.

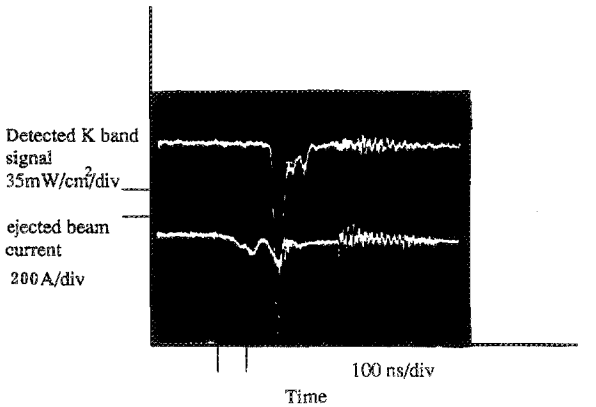

FIG. 2. Typical microwave signal in the K band (top), time coordinated with the ejected beam current (bottom) and associated with the experimental setup in Fig. 1. The detected peak power density is 35 mW/cm^2 (detected power/horn area). The peak current is 200 A and the time scale is 1 div:50 ns.

In the first experiment (see Fig. 1), the electron beam was propagated into a 4 in. diameter drift tube. The microwave emissions were monitored using a series of successively higher frequency directional couplers, bandpass filters and diode detectors. In this run, X band (8–12 GHz) waveguides were used to conduct the signal into the screen room. This signal was separated into the X band (8–12 GHz), Ku band (13–18 GHz), K band (18–26 GHz), and Ka band (26–40 GHz). The voltage of operation was 368 kV. Figure 2 shows a typical microwave signal (K band) time coordinated with the ejected beam current.

Note that the microwave signal is not associated with the initial peak in the current waveform. It was experimentally determined that the initial peak consists of runaway electrons which had left the hollow cathode when there was full anode-cathode voltage.[6] It is well known experimentally[8,9] that the current growth after the initial peak is accompanied by a growing background plasma density. This has been shown in simulations as well.[10] That the microwave emission is associated with the ejected electron beam current in this phase suggests beam-plasma coupling as a mechanism for microwave emission. This will be discussed further in the next section. Figure 3 shows the relative power density in the various bands. Figure 4 illustrates the time evolution of the various bands. In this figure, the central frequency of each band is plotted against the time when emission in this band starts. Note that the power density falls with increasing frequency.

In the second experiment, microwave emissions in the K band were monitored for the various fill gases. Table I shows the measured power density at various charging voltages and for different gases. The variation in operating voltages was due to the varying breakdown voltages of the various gases. From Table I, it is obvious that microwave emission is a function of the gas species. This again suggests the beam plasma interaction as a strong contender for the radiative mechanism because the plasma formation would be influenced by the gas species. Comparing the microwave emission when helium is the fill gas to the case when argon or

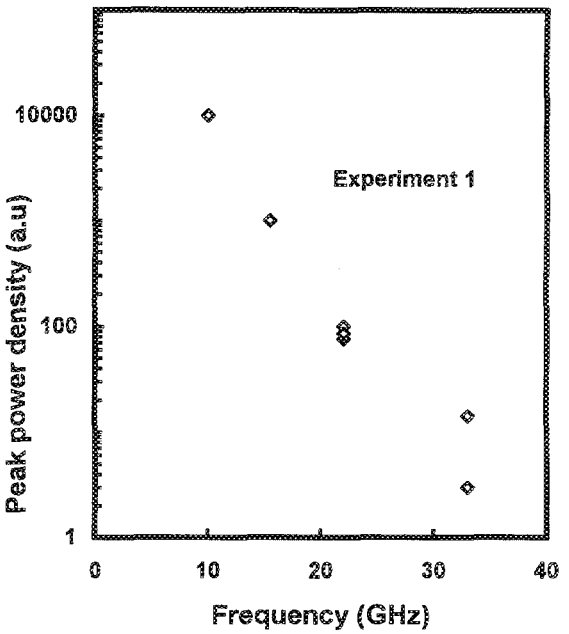

FIG. 3. Relative peak power density (arbitrary units) vs frequency associated with experiment 1 (setup Fig. 1). Note that the frequencies represent the central frequency in each of the various bands. The beam is propagated in the drift tube without any confining structure like a dielectric tube.

neon is used reaffirms previous experimental findings[6] that plasma formation is not as great in the case of helium as in the experiments where argon and neon are used. Note that K band waveguides and a K band low pass filter (HP K362A) were used. A beam collector was used to prevent the beam from hitting the endplate.

In the third series of experiments, relative power emission in the K band was determined as a function of voltage.

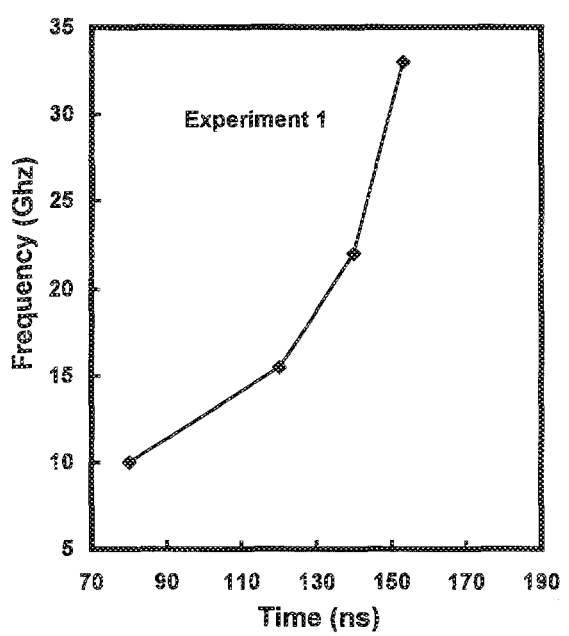

FIG. 4. Time evolution of the central frequencies associated with experiment 1 (setup Fig. 1). No confinement implies that the beam is propagated in the drift tube without any confining structure like a dielectric tube.

TABLE I. Comparison of microwave emissions for various fill gases.

Voltage (charging) (kV)	Gas	Power density (mW/cm^2)	τ_{start} (ns)	τ_{pulse} (ns)
368	neon	99	150	50
368	neon	292	170	50
368	neon	115	140	50
368	helium	16	140	50
316	argon	33	140	50
354	argon	115	140	50

A small diameter (2.54 cm) Pyrex tube was placed in the drift tube to reduce the discharge volume and the confine the plasma formed in the smaller volume. This is shown in Fig. 5. Microwave emissions were monitored in the K band using a K band pipeline. Figure 6 shows the peak power density (arbitrary units) at different voltages for neon. From the figure it appears that the charging voltage has little influence on the microwave emissions in the K band. Typically, the detected peak power density was in the range 95–30 mW/cm^2.The detected peak power densities were comparable to the detected peak power densities in experiments 1 and 2. This suggests that the plasma column is very narrow.

In experiment 4, a polycarbonate (dielectric constant 3.0) drift tube with an inner radius of 0.65 cm and outer radius of 1.77 cm was used to confine the beam plasma system. Figure 7 shows the experimental setup. It was felt that the polycarbonate dielectric tube would be advantageous in the following sense: As the electron beam streams along the dielectric tube, the tube wall becomes negatively charged due to electrons hitting the wall, thus providing initial electrostatic focusing. The small diameter tube also confines the plasma to a smaller cross-sectional area thus increasing the plasma density. Typically, in the case of electron beam-plasma interaction in the absence of a magnetic field, the E_z

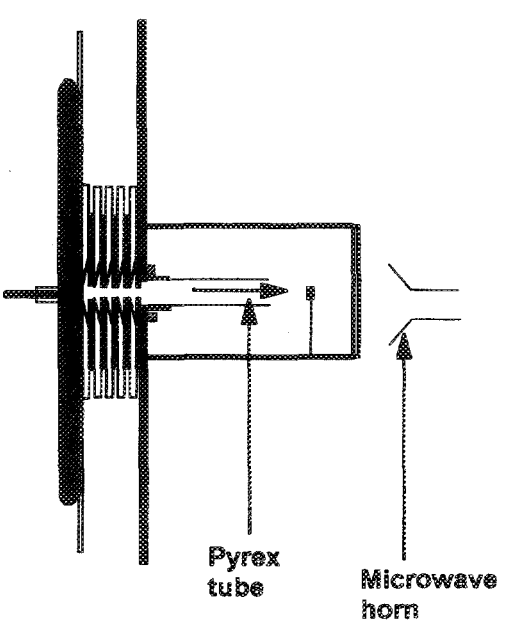

FIG. 5. Experimental setup for experiment 3. A Pyrex tube was used to confine the plasma to ta smaller volume.

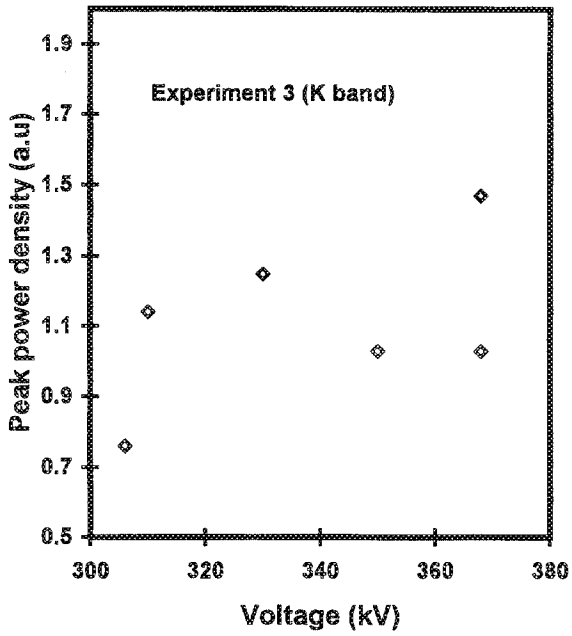

FIG. 6. Microwave emission in the K band at different voltages with Pyrex glass confining the plasma. The detected peak power densities at the K band horn; arbitrary units) are plotted against charging voltages. It appears that the charging voltage has little influence on the power magnitude confirming the fact that the electrons generated later in time have energies much less than the charging voltage equivalent.

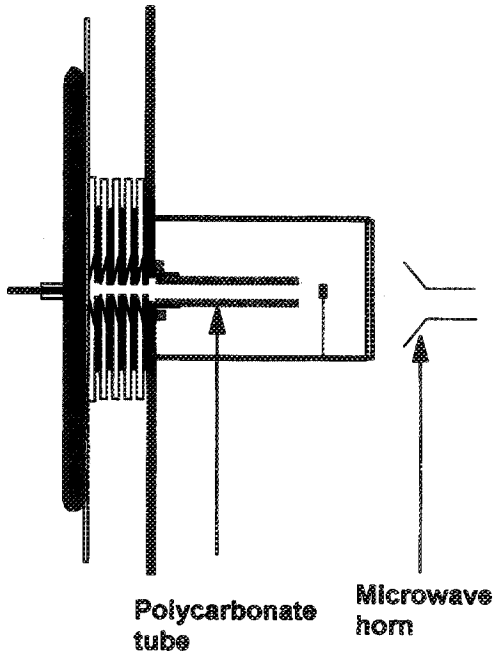

FIG. 7. Experimental setup for experiment 4.

component of the electric field (TM modes) is the strongest at the plasma boundary (surface modes) and declines very rapidly in either direction from the plasma boundary. Thus the power flux is small outside the plasma region. It was hoped that with the use of the thick walled dielectric tube the rapid decline of the electric field would be retarded and the power flux in the dielectric region would increase transforming the surface mode to the volume mode.[11] This would have the effect of releasing the trapped plasma waves. There was significantly higher detected power, but the exact reason behind the increase in the detected power is still not clear.

Figure 8 shows typical shot of microwave emission in the X band. The first burst is associated with the initial peak and the second burst occurs a little later in time (after 100 ns). The peak power density associated with the first burst is 103 W/cm^2 and the peak power density associated with the second burst is 390 W/cm^2. Similar power densities were obtained in subsequent shots. These peak power densities are computed by dividing the detected X band power by the effective horn area (X band). However, the dielectric tube was severely damaged. It appears that the initial burst is due to the interaction of the initial high energy electrons in the waveguide mode. The dielectric tube inserted inside a 2.5 in. conducting cylinder constitutes a slow wave structure. For the electron beam to interact there should be synchronism between beam velocity and the phase velocity of the electromagnetic mode. The following relations should hold:

$$\frac{1}{\beta}=\sqrt{\epsilon}\,,$$

$$\beta=v_z/c, \qquad (1)$$

$\epsilon=$ dielectric constant.

The charging voltage in this experiment was 320.7 kV. This implies that the peak value of β is 0.78. Therefore $1/\beta$ equals 1.26 and $\sqrt{\epsilon=3.0}$ is 1.73. These values are sufficiently close that the stimulated Cherenkov emission cold be a possible mechanism for the observed emissions. This is discussed in the next section. The burst observed later in time is due to beam-plasma interaction. Note that in these measurements X band waveguides were used and an X bandpass filter was used. The X band power density in experiment 1 was 10 W/cm^2. Clearly, confining the beam plasma system to a small cross-sectional area tube improves microwave emission.

In experiment 5, a ceramic tube (dielectric constant 7.0) was introduced in the dielectric tube used in experiment 4. The cross-sectional view is shown in Fig. 9. The inner radius of the ceramic tube is 0.53 cm and the outer radius is 0.65 cm. The polycarbonate extends from 0.65 to 1.77 cm. The purpose of using the ceramic tube was to disturb the syn-

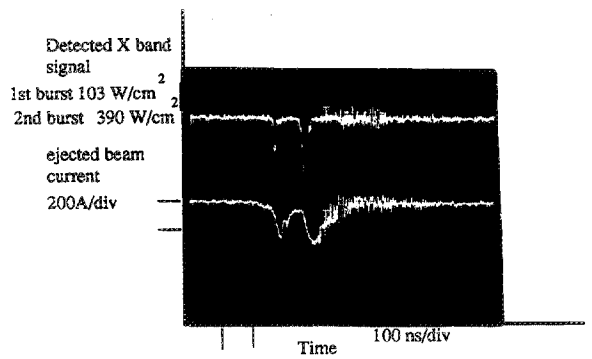

FIG. 8. Microwave emission in X band (first peak 103 W/cm^2, second peak; 390 W/cm^2); Bottom: current (200 A/div). Time scale 100 ns/div.

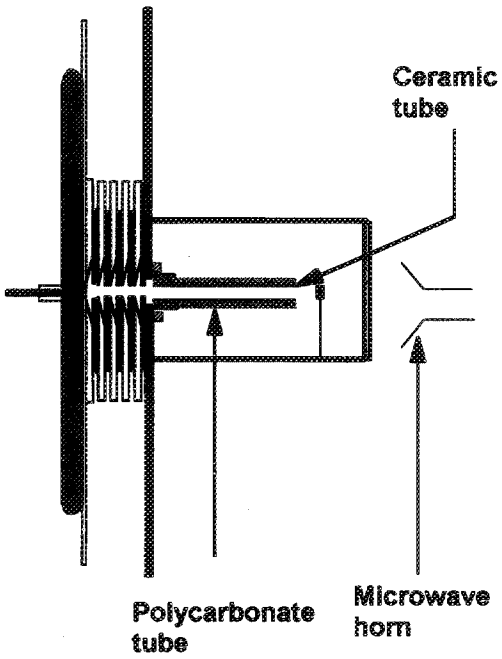

FIG. 9. Experimental setup for experiment 5.

chronism responsible for the Cherenkov emission. Figure 10 shows a typical pulse of radiation in the X band (peak power density is about 8 W/cm^2). In the X band, the peak power density is in the range 4–8 W/cm^2. Again, the peak power densities are computed by dividing the detected power by the effective area of the X band horn. The reason behind the decrease in detected power between experiments 4 and 5 is not clear. There was a single burst with a peak power density at 82 W/cm^2. Note that the microwave burst associated with the initial electrons has disappeared. The voltage in this experiment was in the range 370–376 kV. This implied a $\beta=0.81$ and a $1/\beta=1.5$. This can be attributed to the loss of synchrosnism with the slow wave due to change in the dielectric constant (from 3 to 7). A higher dielectric constant at the beam-dielectric interface would cause a steeper decline of the electric field at the interface. In the K band, the peak power density is between 400 and 2000 mW/cm^2. Figure 11 shows the microwave emission in the X and K band simultaneously. Separate band waveguide pipelines, separate band specific horns, bandpass filters, and detectors were used in

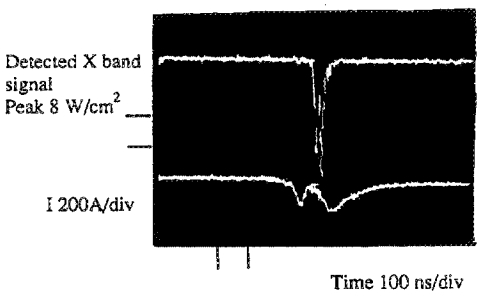

FIG. 10. Top: Microwave emission in X band in a dielectric tube with two materials ($\epsilon_1=7$, $\epsilon_2=3.0$) (experiment 5). The detected peak power density at the X band horn was 8 W/cm^2. Bottom: Ejected electron beam trace (200 A/div): The time scale is 100 ns/div.

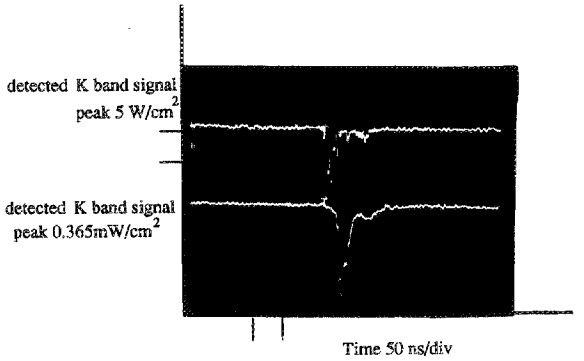

FIG. 11. Microwave emission recorded simultaneously for X and K bands. Top: X band peak power density 5 W/cm^2 (at the horn). Bottom: K band peak power density 0.365 mW/cm^2 at the horn. Note separate band specific components (waveguides, horns, filters and detectors were used). Time scale 100 ns/div.

this experiment. Microwave emissions starts in the X band. It is followed by the K band emission. Note that only X and K bands were monitored in this experiment. Once the X band emission stopped, K band emission began. The detected peak power density recorded in Fig. 11 was 5 W/cm^2 for the X band and 0.365 W/cm^2 for the K band.

Table II summarizes the five experiments for comparison.

IV. DISCUSSION

The electron beam associated with the pseudospark discharge is emitted in two phases—high energy electrons emitted in an earlier stage and the lower energy electrons emitted in a later stage. The experiment described in an earlier section clearly shows that in all cases except one, microwave emissions for the pseudospark discharge were associated with electrons ejected later in time. In experiment 4 (the propagations of the electron beam through polycarbonate) it was observed that in addition to the usual microwave emissions seen with the lower energy electrons there were other emission associated with the initial high energy electrons. The mechanisms behind these microwave bursts will be discussed in the following paragraphs.

A. Initial microwave bursts

The initial electrons of the pseudospark discharge are not associated with any growing background plasma and constitute the runaway electrons at full anode-cathode potential. The fact that the microwave emission is associated with the propagation of these electrons through a polycarbonate tube—a dielectric medium where $\sqrt{\epsilon}$ is close to $1/\beta$ of the beam. This suggests Cherenkov emission as a mechanism of radiation. Here the dielectric acts as a slow wave structure. The disappearance of the radiation when resonance is disrupted as with the ceramic tube in experiment 5 further supports this mechanism. However, further investigation must be carried out before it can be established as the most likely mechanism. Typically, in a dielectric Cherenkov maser the beam is propagated in a strong magnetic field to prevent the beam from hitting the dielectric wall. This would cause the charging of the tube and surface breakdown. In experiment

TABLE II. Comparison of the five microwave related experiments. Note that peaks 1 and 2 refer to the ejected current peaks. The power densities refer to the detected peak power densities at the horn obtained by dividing the detected power by the effective area of the horn.

		Power density (mW/cm^2)						
Exp	V (kV)	X	Ku	K	Ka	Gas	Peak 1	Peak 2
1	268	10×10^3	1×10^3	90	8	Ne		●
2	~368			16–115		He–Ne–Ar		●
3	306–368			95–230		Ne		●
4	320	103×10^3				Ne	●	
		390×10^3						●
5	370	6×10^3		400–2×10 3		Ne		●

4, the e beam was propagated without any magnetic field and the dielectric tube was damaged due to surface breakdown. A beam-surface plasma interaction is not conclusively ruled out. The ceramic tube in experiment 5 was not damaged.

B. Microwave emissions later in time

In all the experiments, microwave emissions were associated with electrons ejected later in time. At this time, the background gas is strongly ionized and there is an ambient plasma. This points to the fact that the mechanism behind the microwave generation may be a beam plasma interaction. In this interaction, the electron beam passing through plasma sets up plasma oscillations[12] (the energy of the electron beam in this experiment is far too low to interact with the electromagnetic modes). The beam intersects with the slow wave modes of the plasma. As a consequence of bounded plasma formation without magnetic field, the plasma is very inhomogeneous, the electric field associated with the plasma oscillations cannot generally be separated into independent longitudinal and transverse components (with respect to the beam direction). This causes the possible subsequent conversion into electromagnetic radiation.[2,13]

The frequency of emission increases with time. The most probable reason is the following. As the beam energy falls, the slope of the beam line in the $w-k_z$ dispersion diagram decreases. The beam line therefore intersects with the plasma mode at higher frequencies. Also, the plasma density is increasing concurrently.

C. Simulation studies

A numerical simulation program developed by Dr. Anatoly Sckvarunets at the Institute for Plasma Research, University of Maryland to study the plasma guide modes (TM) of an electrodynamic system with an inhomogeneous plasma profile was used to determine the intersection points of the beam line with slow plasma modes. This study was carried out to determine the range of plasma densities and the frequencies for which intersection was possible.

The profile of the plasma density for which the investigation was carried out is shown in Fig. 12. The plasma profile was made small in diameter to generate the pinched beam plasma column with which the late time microwave emissions was associated.

This numerical investigation was carried out in the following manner. The simulation was carried out in two loops. In the outer loop the beam energy was fixed. In the inner loop the plasma density at the peak was fixed and the frequency was swept from the peak plasma frequency downwards for which a solution (the intersection of the beam line with a plasma mode) was obtained. The highest frequency solution was chosen. Note that the TM mode was studied because it was felt that the electron beam with its greater energy in the longitudinal direction would interact most strongly with a TM mode (E_z component). Once the inner loop was completed, the plasma density is changed and the inner loop was repeated to determine new solutions. The plasma densities (peak) and the corresponding plasma frequencies (peak) for which the study was carried out are shown in Table III.

Once the solutions were determined for all the plasma densities, the energy of the electron beam was varied. This study was carried out for electron beams with energies 50–100, 200, and 360 keV (full charging voltage). In Fig. 13, the

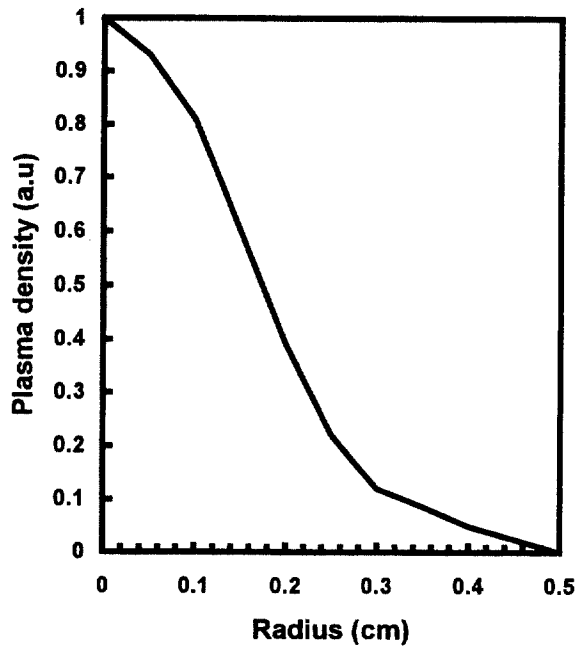

FIG. 12. Assumed plasma profile for numerical calculation. Plasma density is shown in arbitary units. Note the plasma profile was assumed in this manner because the pseudospark generated electron beam has a diameter in the range 1.5–0.5 mm for lower energy electrons.

TABLE III. Peak plasma density and corresponding peak plasma frequency.

Peak plasma density 10^{12}/cm^3	Peak plasma frequency GHz
6.4	22.71
7.2	24.09
8.0	25.39
8.8	26.63
9.6	27.82
11.1	29.91
13.3	32.74
15.5	35.35
17.7	37.78
19.9	40.05
21.0	41.15

highest frequencies for which a solution exists (intersection of the beam line and plasma mode) are plotted against the peak plasma densities for various energies of the electron beams. It is clear for the diagram that for higher frequencies, only electrons with low (50–100 keV) energies have solutions for plasma densities in the range $6-20\times10^{12}$ cm^{-3}. For lower frequencies, all the electron beams (50, 100, 200, and 360 keV) have solutions. However, for electrons of energies 200 and 360 keV, the plasma densities have to be greater than 1×10^{13} cm^{-3}. Since the lower frequencies (X band) are generated early in time, and the electron beams have higher energies, the plasma densities should be of the order of $1-2\times10^{13}$ cm^{-3}. As the plasma density increases and the beam energies fall, the microwave emission shifts to higher frequencies.

The numerical studies while by no means exhaustive, support electron beam-plasma interaction for plasma densities in the range $1-2\times10^{13}$ cm^{-3} with falling beam energies (with time) a possible mechanism for the microwave signature accompanying the psuedospark discharge. A further confirmation of the plasma densities can be made by comparing the electron beam density with the electron current at lower energy 240 keV is of the order 240 A.[6] The diameter of the electron beam varies with the energy. The initial higher energy electrons have a diameter of the order 3–4 mm and the self-pinched lower energy electrons have a diameter of the order of 0.5 mm.[6] Using 1.5 mm as an estimate of the diameter of electron beam of energy 200 keV, the beam density was calculated to be $\sim1.62\times10^{13}$ cm^{-3}. This is comparable to the peak plasma density.

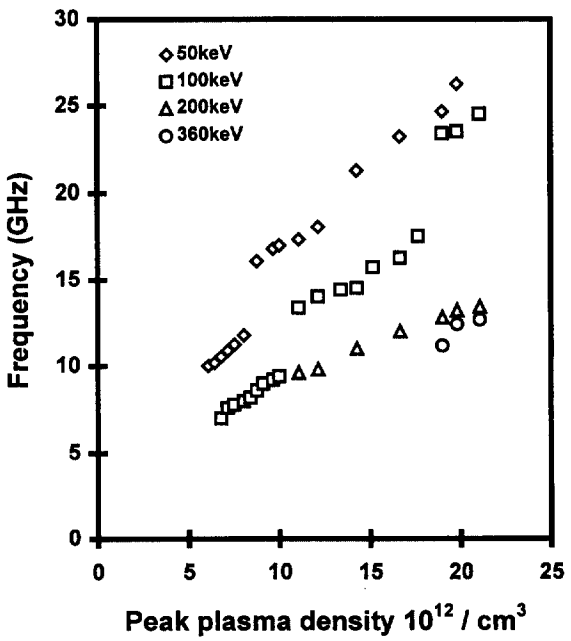

FIG. 13. Highest frequency solutions (intersection of the beam line with a plasma mode) vs peak plasma density for electron beams with different energies.

V. CONCLUSIONS

An initial set of five experiments were conducted to investigate microwave emissions from a multistack pseudospark device. The generation of the microwaves in all cases but one (experiment 4) was attributed to an electrons beam-plasma interaction. The microwave emission in these experiments were associated with lower energy electrons emitted later. In the case of experiment 4 (propagation of electrons through a polycarbonate tube), microwave emissions were associated with the initial electrons in addition to the bursts seen later in time. Cherenkov emission was suggested as a possible mechanism of generation. However, further investigations need to be carried out before it can be established as the most likely mechanism of generation.

These are preliminary experiments. Further work has been planned to carry out a more detailed study of the beam-plasma interaction. The issue of higher detected power densities in the case of beam passage through a dielectric tube will be studied using both simulation and experimentation.

ACKNOWLEDGMENTS

The authors would like to acknowledge useful discussions with Anatoly Skhavarunetz and Girish Saraph. It is also a pleasure to acknowledge the technical support of Jay Pyle and Doug Cohen. This work was supported by the U.S. Department of Energy.

[1] J. Christiansen and Ch. Schulthheiss, Z. Phys. A **2990**, 35 (1979).
[2] V. P. Popovich, J. P. Kharchenko, and E. G. Shustin, Radiotekh. Elektron. **18**, 649 (1973).
[3] S. Jordan, A. Ben-Amar Baranga, G. Benford, D. Tzach, and K. Kato, Phys. Fluids **28**, 366 (1985).
[4] M. V. Kuzelev, A. A. Ruhkahdze, P. S. Strelkov, and A. G. Shkvarunets, Sov. J. Plasma Phys. **13**, 793 (1987).
[5] K. Ramaswamy, W. W. Destler, Z. Segalov, and J. Rodgers, J. Appl. Phys. **75**, 4432 (1994).
[6] K. Ramaswamy, W. W. Destler, and J. Rodgers, J. Appl. Phys. **80**, 4887 (1996).
[7] R. Liou *et al.*, Proc. IEDM 29 (1990).
[8] M. Stretter, P. Felsner, J. Christiansen, K. Frank, A. Gortler, G. Hintz, T. Mehr, R. Stark, and R. Tkotz, IEEE Trans. Plasma Sci. **PS-23**, 283 (1995).
[9] R. Stark, J. Christiansen, K. Frank, F. Mucke, and M. Stetter, IEEE Trans. Plasma Sci. **PS-23**, 258 (1995).
[10] J. P. Boeuf and L. C. Pitchford, IEEE Trans. Plasma Sci. **PS-19**, 286 (1991).
[11] A. Shkvarunets (private communication).
[12] Ya. B. Fainberg, At. Energ. **11**, 313 (1961).
[13] D. A. Tidman and G. H. Weiss, Phys. Fluids **4**, 703 (1961).